Journal of Science and Technology in Civil Engineering NUCE 2020. 14 (1): 42–53

BENDING AND FREE VIBRATION BEHAVIORS OF COMPOSITE PLATES USING THE C^0-HSDT BASED FOUR-NODE ELEMENT WITH IN-PLANE ROTATIONS

Huynh Huu Tai[a], Nguyen Van Hieu[a,*], Vu Duy Thang[b]

[a] *Faculty of Civil Engineering, Ho Chi Minh City University of Architecture, 196 Pasteur street, District 3, Ho Chi Minh City, Vietnam*
[b] *Faculty of Civil Engineering, Mien Tay Construction University, 20B Pho Co Dieu street, District 3, Vinh Long City, Vietnam*

Article history:
Received 22/08/2019, Revised 01/10/2019, Accepted 01/10/2019

Abstract

In this paper the smoothed four-node element with in-plane rotations MISQ24 is combined with a C^0-type higher-order shear deformation theory (C^0-HSDT) to propose an improved linear quadrilateral plate element for static and free vibration analyses of laminated composite plates. This improvement results in two additional degrees of freedom at each node and require no shear correction factors while ensuring the high precision of numerical solutions. Composite plates with different lay-ups, boundary conditions and various geometries such as rectangular, skew and triangular plates are analyzed using the proposed element. The obtained numerical results are compared with those from previous studies in the literature to demonstrate the effectiveness, the reliability and the accuracy of the present element.

Keywords: composite laminated plates; bending problems; free vibration; C^0-HSDT; MISQ24.

https://doi.org/10.31814/stce.nuce2020-14(1)-04

1. Introduction

In recent years, many building construction not only ensure the working ability of structure but also require that the architecture must be aesthetic. In practice, plate texture or plate shape are widely used in lots of building constructions for different objectives such as crediting the cover to protect construction, enhancing theory of art, increasing the resistance to heat and joined forces... Therefore, finding more efficient calculations method along with high reliability in analysis of plate structures design is always essential needed. In recent years, structures made of composite materials have been using intensively in aerospace, marine and civil infrastructure, etc., because they possess many favorable mechanical properties such as high stiffness to weight and low density.

Among the plate theories [1–4], the higher-order shear deformation theory (HSDT) is widely used because it does not need shear correction factors and gives accurate transverse shear stresses. However, the need of C^1-continuous approximation for the displacement fields in the HSDT with lower-order finite element models cause some obstacles. To overcome these shortcomings, Shankara and Iyengar [5] develop a revised form of HSDT which only requires C^0 continuity for displacement

*Corresponding author. *E-mail address:* hieu.nguyenvan@uah.edu.vn (Hieu, N. V.)

fields (C^0 -HSDT). In the C^0-HSDT, two additional variables have been added, and hence only the first derivative of transverse displacements is required.

This paper presents a novel numerical procedure based on four-node element MISQ24 with in-plane rotations [6] associated with the C^0-HSDT type for static and free vibration analyses of laminated composite plates. The higher-order shear deformation plate theory is involved in the formulation in order to avoid using the shear correction factors and to improve the accuracy of transverse shear stresses. In the present method, the membrane and bending strains are smoothed over sub-quadrilateral domains of elements. As a result, the membrane and bending stiffness matrices are integrated along the boundary of the smoothing domains instead of over the element surfaces. And the shear stiffness matrix is based on reduced-integration technique to remove the shear-locking phenomenon. Compared with the conventional finite element methods, the present approach requires more computational time for the gradient matrices of the membrane and bending strains when more than one smoothing domain are employed. However, the present formulation uses only linear approximations and its implementation into finite element programs using Matlab programming is quite simple. Several numerical examples are given to show the performance of the proposed method and results obtained are compared to other published methods in the literature.

2. C^0-HSDT and the weak form for plate model

Let Ω be the domain in R^2 occupied by the mid-plane of the plate. The displacements of an arbitrary point in the plate are expressed as [5]

$$\begin{aligned} u(x,y,z) &= u_0 + \left(z - \frac{4z^3}{3h^2}\right)\theta_y - \frac{4z^3}{3h^2}\varphi_x \\ v(x,y,z) &= v_0 - \left(z - \frac{4z^3}{3h^2}\right)\theta_x - \frac{4z^3}{3h^2}\varphi_y \\ w(x,y,0) &= w_0 \end{aligned} \qquad \left(-\frac{h}{2} \le z \le \frac{h}{2}\right) \tag{1}$$

where u_0, v_0 and w_0 are axial and transverse displacements at the mid-surface of the plates, respectively; $\varphi_x, \varphi_y, \theta_x, \theta_y$ are rotations due to the bending and shear effects. It can be seen that the present theory is composed of seven unknowns: three axial and transverse displacements, four rotations with respect to the y- and x-axis as shown in Fig. 1.

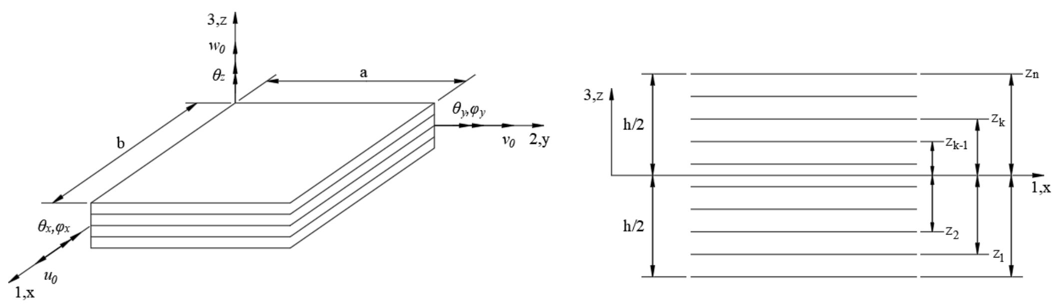

Figure 1. Composite plate

In-plane strains are expressed by the following equation:

$$\boldsymbol{\varepsilon}_p = \begin{bmatrix} \varepsilon_{xx} & \varepsilon_{yy} & \gamma_{xy} \end{bmatrix}^T = \boldsymbol{\varepsilon}_0 + z\boldsymbol{\kappa}_1 - \frac{4}{3h^2}z^3\boldsymbol{\kappa}_2 \tag{2}$$

where the membrane strains are obtained from the symmetric displacement gradient

$$\boldsymbol{\varepsilon}_0 = \left\{ \begin{array}{c} \dfrac{\partial u_0}{\partial x} \\ \dfrac{\partial v_0}{\partial y} \\ \dfrac{\partial u_0}{\partial y} + \dfrac{\partial v_0}{\partial x} \end{array} \right\} \tag{3}$$

and the bending strains are given by

$$\boldsymbol{\kappa}_1 = \begin{bmatrix} \theta_{y,x} \\ -\theta_{x,y} \\ \theta_{y,y} - \theta_{x,x} \end{bmatrix}, \quad \boldsymbol{\kappa}_2 = \begin{bmatrix} \theta_{y,x} + \varphi_{x,x} \\ -\theta_{x,y} + \varphi_{y,y} \\ \left(\theta_{y,y} - \theta_{x,x}\right) + \left(\varphi_{x,y} + \varphi_{y,x}\right) \end{bmatrix} \tag{4}$$

The transverse shear strain vector is given as

$$\boldsymbol{\gamma} = \begin{bmatrix} \gamma_{xz} & \gamma_{yz} \end{bmatrix}^T = \boldsymbol{\varepsilon}_s + z^2 \boldsymbol{\kappa}_s \tag{5}$$

in which

$$\boldsymbol{\varepsilon}_s = \begin{bmatrix} w_x + \theta_y \\ w_y - \theta_x \end{bmatrix}, \quad \boldsymbol{\kappa}_s = -\frac{4}{h^2} \begin{bmatrix} \varphi_x + \theta_y \\ \varphi_y - \theta_x \end{bmatrix} \tag{6}$$

The composite plate is usually made of several orthotropic layers in which the stress–strain relation for the k^{th} orthotropic lamina with the arbitrary fiber orientation maps to the reference as

$$\left\{ \begin{array}{c} \sigma_{xx} \\ \sigma_{yy} \\ \sigma_{xy} \\ \tau_{xz} \\ \tau_{yz} \end{array} \right\}^{(k)} = \begin{bmatrix} \overline{Q}_{11} & \overline{Q}_{12} & \overline{Q}_{16} & 0 & 0 \\ \overline{Q}_{21} & \overline{Q}_{22} & \overline{Q}_{26} & 0 & 0 \\ \overline{Q}_{61} & \overline{Q}_{62} & \overline{Q}_{66} & 0 & 0 \\ 0 & 0 & 0 & \overline{Q}_{55} & \overline{Q}_{54} \\ 0 & 0 & 0 & \overline{Q}_{45} & \overline{Q}_{44} \end{bmatrix}^{(k)} \left\{ \begin{array}{c} \varepsilon_{xx} \\ \varepsilon_{yy} \\ \varepsilon_{xy} \\ \gamma_{xz} \\ \gamma_{yz} \end{array} \right\}^{(k)} \tag{7}$$

where $\overline{Q}_{ij}$ $(i, j = 1, 2, 4, 5, 6)$ are the material constants of k^{th} layer in global coordinate system. Under weak form, the normal forces, bending moments, higher-order moments, shear forces and higher-order shear forces can then be computed through the following relations

$$\left\{ \begin{array}{c} \mathbf{N} \\ \mathbf{M} \\ \mathbf{P} \\ \mathbf{Q} \\ \mathbf{R} \end{array} \right\} = \begin{bmatrix} \mathbf{A} & \mathbf{B} & c_1\mathbf{E} & 0 & 0 \\ \mathbf{B} & \mathbf{D} & c_1\mathbf{F} & 0 & 0 \\ c_1\mathbf{E} & c_1\mathbf{F} & c_1^2\mathbf{H} & 0 & 0 \\ 0 & 0 & 0 & \mathbf{G} & c_2\mathbf{S} \\ 0 & 0 & 0 & c_2\mathbf{S} & c_2^2\mathbf{T} \end{bmatrix} \left\{ \begin{array}{c} \boldsymbol{\varepsilon}_0 \\ \boldsymbol{\kappa}_1 \\ \boldsymbol{\kappa}_2 \\ \boldsymbol{\varepsilon}_s \\ \boldsymbol{\kappa}_s \end{array} \right\} = \begin{bmatrix} \mathbf{D}_{bm} & 0 \\ 0 & \mathbf{D}_s \end{bmatrix} \boldsymbol{\varepsilon}'' \tag{8}$$

with

$$(\mathbf{A}, \mathbf{B}, \mathbf{D}, \mathbf{E}, \mathbf{F}, \mathbf{H}) = \int_{-h/2}^{h/2} \left(1, z, z^2, z^3, z^4, z^6\right) \overline{Q}_{ij} dzi, \, j = 1, 2, 6 \tag{9}$$

$$(\mathbf{G}, \mathbf{S}, \mathbf{T}) = \int_{-h/2}^{h/2} \left(1, z^2, z^4\right) \overline{Q}_{ij} dzi, \, j = 4, 5 \tag{10}$$

and the parameters

$$c_1 = -\frac{4}{3h^2}, \quad c_2 = -\frac{4}{h^2} \tag{11}$$

A weak form of the static model for laminated composite plates can be briefiy expressed as:

$$\int_\Omega \delta\boldsymbol{\varepsilon}_p^T \mathbf{D}_{bm} \boldsymbol{\varepsilon}_p d\Omega + \int_\Omega \delta\boldsymbol{\gamma}^T \mathbf{D}_s \boldsymbol{\gamma} d\Omega = \int_\Omega \delta w p d\Omega \tag{12}$$

where p is the transverse loading per unit area and strain components $\boldsymbol{\varepsilon}_p$ and $\boldsymbol{\gamma}$ are expressed by

$$\boldsymbol{\varepsilon}_p = \left\{ \begin{array}{ccc} \boldsymbol{\varepsilon}_0 & \boldsymbol{\kappa}_1 & \boldsymbol{\kappa}_2 \end{array} \right\}^T, \quad \boldsymbol{\gamma} = \left\{ \begin{array}{cc} \boldsymbol{\varepsilon}_s & \boldsymbol{\kappa}_s \end{array} \right\}^T \tag{13}$$

For the free vibration analysis, a weak form of composite plates can be derived from the following dynamic equation

$$\int_\Omega \delta\boldsymbol{\varepsilon}_p^T \mathbf{D}_{bm} \boldsymbol{\varepsilon}_p d\Omega + \int_\Omega \delta\boldsymbol{\gamma}^T \mathbf{D}_s \boldsymbol{\gamma} d\Omega = \int_\Omega \delta\mathbf{u}^T \mathbf{m}\ddot{\mathbf{u}} d\Omega \tag{14}$$

where **m** is defined as:

$$\mathbf{m} = \begin{bmatrix} I_1 & 0 & 0 & I_2 & 0 & 0 & c_1/3I_4 & 0 \\ & I_1 & 0 & 0 & I_2 & 0 & 0 & c_1/3I_4 \\ & & I_1 & 0 & 0 & I_2 & 0 & 0 \\ & & & I_3 & 0 & 0 & c_1/3I_5 & 0 \\ & & & & I_3 & 0 & 0 & c_1/3I_5 \\ & & & & & I_3 & 0 & 0 \\ & & & & & & c_1^2/9I_7 & 0 \\ & sym & & & & & & c_1^2/9I_7 \end{bmatrix} \tag{15}$$

with

$$(I_1, I_2, I_3, I_4, I_5, I_7) = \int_{-t/2}^{t/2} \rho \left(1, z, z^2, z^3, z^4, z^6\right) dz \tag{16}$$

3. A formulation of four-node quadrilateral plate element

Discretize the bounded domain Ω of plates into N_c finite elements such that $\Omega = \cup_{c=1}^{N_c} \Omega_c$ and $\Omega_i \cap \Omega_j = \emptyset$ with $i \neq j$. The displacement field **u** of the standard finite element solution using the four-node with in-plane rotations can be approximated by

$$\mathbf{u} = \sum_{i=1}^{N_n} \begin{bmatrix} N_i & 0 & 0 & 0 & 0 & 0 & 0 & 0 \\ 0 & N_i & 0 & 0 & 0 & 0 & 0 & 0 \\ 0 & 0 & N_i & 0 & 0 & 0 & 0 & 0 \\ 0 & 0 & 0 & N_i & 0 & 0 & 0 & 0 \\ 0 & 0 & 0 & 0 & N_i & 0 & 0 & 0 \\ 0 & 0 & 0 & 0 & 0 & N_i & 0 & 0 \\ 0 & 0 & 0 & 0 & 0 & 0 & N_i & 0 \\ 0 & 0 & 0 & 0 & 0 & 0 & 0 & N_i \end{bmatrix} \mathbf{q}_i \tag{17}$$

where N_n is the total number of nodes of the mesh, $N_i = \frac{1}{4}(1 + \xi_i \xi)(1 + \eta_i \eta)$ is the shape function of the four-node serendipity element, $\mathbf{q}_i^T = \left[\begin{array}{cccccccc} u & v & w & \theta_x & \theta_y & \theta_z & \varphi_x & \varphi_y \end{array} \right]$ is the displacement vector of the nodal degrees of freedom of $\mathbf{u}$ associated to the i^{th} node, respectively. The membrane, bending and shear strains can be then expressed in the matrix forms as

$$\begin{gathered}\boldsymbol{\varepsilon}_0 = \sum_i \mathbf{B}_i^m \mathbf{q}_i; \quad \boldsymbol{\kappa}_1 = \sum_i \mathbf{B}_{1i}^b \mathbf{q}_i; \quad \boldsymbol{\kappa}_2 = \sum_i \mathbf{B}_{2i}^b \mathbf{q}_i \\ \boldsymbol{\varepsilon}_s = \sum_i \mathbf{B}_{0i}^s \mathbf{q}_i; \quad \boldsymbol{\kappa}_s = \sum_i \mathbf{B}_{1i}^s \mathbf{q}_i\end{gathered} \tag{18}$$

where

$$\mathbf{B}_i^m = \begin{bmatrix} N_{i,x} & 0 & 0 & 0 & 0 & 0 & 0 & 0 \\ 0 & N_{i,y} & 0 & 0 & 0 & 0 & 0 & 0 \\ N_{i,y} & N_{i,x} & 0 & 0 & 0 & 0 & 0 & 0 \end{bmatrix} \tag{19}$$

$$\mathbf{B}_{1i}^b = \begin{bmatrix} 0 & 0 & 0 & 0 & N_{i,x} & 0 & 0 & 0 \\ 0 & 0 & 0 & -N_{i,y} & 0 & 0 & 0 & 0 \\ 0 & 0 & 0 & -N_{i,x} & N_{i,y} & 0 & 0 & 0 \end{bmatrix} \tag{20}$$

$$\mathbf{B}_{2i}^b = \begin{bmatrix} 0 & 0 & 0 & 0 & N_{i,x} & 0 & N_{i,x} & 0 \\ 0 & 0 & 0 & -N_{i,y} & 0 & 0 & 0 & N_{i,y} \\ 0 & 0 & 0 & -N_{i,x} & N_{i,y} & 0 & N_{i,y} & N_{i,x} \end{bmatrix} \tag{21}$$

$$\mathbf{B}_{0i}^s = \begin{bmatrix} 0 & 0 & N_{i,x} & 0 & N_i & 0 & 0 & 0 \\ 0 & 0 & N_{i,y} & -N_i & 0 & 0 & 0 & 0 \end{bmatrix} \tag{22}$$

$$\mathbf{B}_{1i}^s = \begin{bmatrix} 0 & 0 & 0 & 0 & N_i & 0 & N_i & 0 \\ 0 & 0 & 0 & -N_i & 0 & 0 & 0 & N_i \end{bmatrix} \tag{23}$$

As shown in Fig. 2, a quadrilateral element domain Ω_c is further divided into nc smoothing cells. The generalized strain field is smoothed by a weighted average of the original generalized strains using the strain smoothing operation for each smoothing cell as follows

$$\tilde{\boldsymbol{\varepsilon}}(x_C) = \int_{\Omega_C} \boldsymbol{\varepsilon}(x)\Phi(x - x_C)\, d\Omega \tag{24}$$

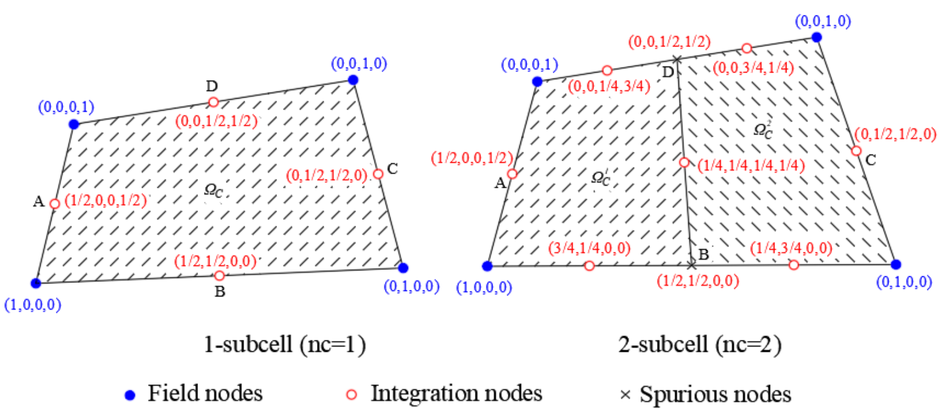

Figure 2. Subdivision of an element into *nc* cells and the values of shape functions at nodes [6]

Introducing the approximation of the linear membrane strain by the quadrilateral finite element using Allman-type interpolation functions with drilling degrees of freedom [7] and applying the divergence theorem, the smoothed membrane strain can be obtained as

$$\tilde{\boldsymbol{\varepsilon}} = \frac{1}{A_c}\int_{\Gamma_c}\mathbf{n}(\mathbf{x})\mathbf{u}(\mathbf{x})d\Gamma = \frac{1}{A_c}\int_{\Gamma_c}\sum_{i=1}^{4}\mathbf{n}(\mathbf{x})\mathbf{N}_i(\mathbf{x})\mathbf{q}_i d\Gamma = \sum_{i=1}^{4}\tilde{\mathbf{B}}_i^m\mathbf{q}_i \tag{25}$$

where

$$\tilde{\boldsymbol{B}}_i^m(x_C) = \frac{1}{A_C}\int_{\Gamma_C}\begin{pmatrix} N_i n_x & 0 & 0 & 0 & 0 & Nx_i n_x \\ 0 & N_i n_y & 0 & 0 & 0 & Ny_i n_y \\ N_i n_y & N_i n_x & 0 & 0 & 0 & Nx_i n_y + Ny_i n_x \end{pmatrix} \tag{26}$$

In which $\mathbf{q}_i = \begin{bmatrix} u & v & w & \theta_x & \theta_y & \theta_z \end{bmatrix}$ is the nodal displacement vector; Nx_i and Ny_i are Allman' s incompatible shape functions defined in [7], and n_x and n_y are the components of the outward unit vector n normal to the boundary Γ_C.

Applying Gauss integration along with four segments of the boundary Γ_C of the smoothing domain Ω_C, the above equation can be rewritten in algebraic form as

$$\begin{aligned}\tilde{\boldsymbol{B}}_i^m(x_C) = {} & \frac{1}{A_C}\sum_{m=1}^{ns}\begin{pmatrix} \sum_{n=1}^{nG} w_n N_i(x_{mn}) n_x & 0 & 0 \\ 0 & \sum_{n=1}^{nG} w_n N_i(x_{mn}) n_y & 0 \\ 0 & \sum_{n=1}^{nG} w_n N_i(x_{mn}) n_y & 0 \\ \sum_{n=1}^{nG} w_n N_i(x_{mn}) n_y & \sum_{n=1}^{nG} w_n N_i(x_{mn}) n_x & 0 \end{pmatrix} \\ & + \frac{1}{A_C}\sum_{m=1}^{ns}\begin{pmatrix} 0 & 0 & \sum_{n=1}^{nG} w_n Nx_i(x_{mn}) n_x \\ 0 & 0 & \sum_{n=1}^{nG} w_n Ny_i(x_{mn}) n_y \\ 0 & 0 & \sum_{n=1}^{nG} w_n Nx_i(x_{mn}) n_y + \sum_{n=1}^{nG} w_n Ny_i(x_{mn}) n_x \end{pmatrix}\end{aligned} \tag{27}$$

where nG is the number of Gauss integration points, $\mathbf{x}_{mn}$ is the Gauss point and ω_n is the corresponding weighting coefficients. The first term in Eq. (27), which relates to the in-plane translations (approximated by bilinear shape functions), is evaluated by one Gauss point ($nG = 1$). The second term, associated with the in-plane rotations (approximated by quadratic shape functions), is computed using two Gauss points ($nG = 2$).

The smoothed membrane element stiffness matrix can be obtained as

$$\tilde{\mathbf{K}} = \tilde{\mathbf{K}}_m + \mathbf{P}_\gamma = \int_\Omega \tilde{\mathbf{B}}_i^{mT}\mathbf{A}\tilde{\mathbf{B}}_i^m d\Omega + \gamma\int_\Omega \mathbf{b}^T\mathbf{b}d\Omega = \sum_{C=1}^{nc}\tilde{\mathbf{B}}_{iC}^{mT}\mathbf{A}\tilde{\mathbf{B}}_{iC}^m A_C + \gamma\int_\Omega \mathbf{b}^T\mathbf{b}d\Omega \tag{28}$$

in which nc is the number of smoothing cells. To avoid numerically over-stiffening the membrane, one smoothing cell ($nc = 1$) is used in the present formulation. Higher numbers of smoothing cells will lead to stiffer solutions and the accuracy may not be enhanced considerably. The penalty matrix $\mathbf{P}_\gamma$ is integrated using a 1- point Gauss quadrature to suppress a spurious, zero-energy mode associated with the drilling DOFs. The positive penalty parameter γ is chosen as $\gamma/G_{12} = 1/1000$ in the study.

The smoothed bending element stiffness matrix can be obtained using the similar procedure [6] and finally, the element tangent stiffness matrix is modified as

$$\tilde{\mathbf{K}} = \tilde{\mathbf{K}}_m + \tilde{\mathbf{K}}_{mb} + \tilde{\mathbf{K}}_{mb}^T + \tilde{\mathbf{K}}_b + \tilde{\mathbf{K}}_s \tag{29}$$

where

$$\tilde{\mathbf{K}}_m = \int_\Omega \tilde{\mathbf{B}}_i^{mT}\mathbf{A}\tilde{\mathbf{B}}_i^m d\Omega + \gamma\int_\Omega \mathbf{b}^T\mathbf{b}d\Omega = \sum_{C=1}^{nc}\tilde{\mathbf{B}}_i^{mCT}\mathbf{A}\tilde{\mathbf{B}}_i^{mC}A_C + \gamma\int_\Omega \mathbf{b}^T\mathbf{b}d\Omega \tag{30}$$

$$\begin{aligned}\tilde{\mathbf{K}}_{mb} &= \int_\Omega\left(\tilde{\mathbf{B}}_i^{mT}\mathbf{B}\tilde{\mathbf{B}}_{1i}^b + c_1\tilde{\mathbf{B}}_i^{mT}\mathbf{E}\tilde{\mathbf{B}}_{2i}^b + \tilde{\mathbf{B}}_{1i}^{bT}\mathbf{B}\tilde{\mathbf{B}}_i^m + c_1\tilde{\mathbf{B}}_{2i}^{bT}\mathbf{E}\tilde{\mathbf{B}}_i^m\right)d\Omega \\ &= \sum_{C=1}^{1}\left(\tilde{\mathbf{B}}_i^{mCT}\mathbf{B}\tilde{\mathbf{B}}_{1i}^{bC} + c_1\tilde{\mathbf{B}}_i^{mCT}\mathbf{E}\tilde{\mathbf{B}}_{2i}^{bC} + \tilde{\mathbf{B}}_{1i}^{bCT}\mathbf{B}\tilde{\mathbf{B}}_i^{mC} + c_1\tilde{\mathbf{B}}_{2i}^{bCT}\mathbf{E}\tilde{\mathbf{B}}_i^{mC}\right)A_C\end{aligned} \tag{31}$$

$$\begin{aligned}\tilde{\mathbf{K}}_b &= \int_\Omega\left(\tilde{\mathbf{B}}_{1i}^{bT}\mathbf{D}\tilde{\mathbf{B}}_{1i}^b + c_1\tilde{\mathbf{B}}_{1i}^{bT}\mathbf{F}\tilde{\mathbf{B}}_{2i}^b + c_1\tilde{\mathbf{B}}_{2i}^{bT}\left(\tilde{\mathbf{B}}_{1i}^b + c_1^2\tilde{\mathbf{B}}_{2i}^{bT}\mathbf{H}\tilde{\mathbf{B}}_{2i}^b\right)d\Omega \\ &= \sum_{C=1}^{2}\left(\tilde{\mathbf{B}}_{1i}^{bCT}\mathbf{D}\tilde{\mathbf{B}}_{1i}^{bC} + c_1\tilde{\mathbf{B}}_{1i}^{bCT}\mathbf{F}\tilde{\mathbf{B}}_{2i}^{bC} + c_1\tilde{\mathbf{B}}_{2i}^{bCT}\mathbf{F}\tilde{\mathbf{B}}_{1i}^{bC} + c_1^2\tilde{\mathbf{B}}_{2i}^{bCT}\mathbf{H}\tilde{\mathbf{B}}_{2i}^{bC}\right)A_C\end{aligned} \tag{32}$$

$$\begin{aligned}\tilde{\mathbf{K}}_s &= \int_\Omega\left(\mathbf{B}_{0i}^{sT}\mathbf{G}\mathbf{B}_{0i}^s + c_2\mathbf{B}_{0i}^{sT}\mathbf{S}\mathbf{B}_{1i}^s + c_2\mathbf{B}_{1i}^{sT}\mathbf{s}\mathbf{B}_{0i}^s + c_2^2\mathbf{B}_{1i}^{sT}\mathbf{T}\mathbf{B}_{1i}^s\right)d\Omega \\ &= \sum_{i=1}^{2}\sum_{j=1}^{2}w_iw_j\left(\mathbf{B}_{0i}^{sT}\mathbf{G}\mathbf{B}_{0i}^s + c_2\mathbf{B}_{0i}^{sT}\mathbf{S}\mathbf{B}_{1i}^s + c_2\mathbf{B}_{1i}^{sT}\mathbf{S}\mathbf{B}_{0i}^s + c_2^2\mathbf{B}_{1i}^{sT}\mathbf{T}\mathbf{B}_{1i}^s\right)|\mathbf{J}|\,d\xi d\eta\end{aligned} \tag{33}$$

with

$$\mathbf{b}_i = \begin{bmatrix} -\frac{1}{2}N_{i,y} & \frac{1}{2}N_{i,x} & -\frac{1}{2}\left(Nx_{i,y} + Ny_{i,x}\right) - N_i \end{bmatrix} \tag{34}$$

$$\tilde{\mathbf{B}}_{1i}^b = \frac{1}{A_C}\sum_{b=1}^{4}\begin{pmatrix} 0 & 0 & 0 & 0 & N_in_x & 0 & 0 & 0 \\ 0 & 0 & 0 & -N_in_y & 0 & 0 & 0 & 0 \\ 0 & 0 & 0 & -N_in_x & N_in_y & 0 & 0 & 0 \end{pmatrix} l_b \tag{35}$$

$$\tilde{\mathbf{B}}_{2i}^b = \frac{1}{A_C}\sum_{b=1}^{4}\begin{pmatrix} 0 & 0 & 0 & 0 & N_in_x & 0 & N_in_x & 0 \\ 0 & 0 & 0 & -N_in_y & 0 & 0 & 0 & N_in_y \\ 0 & 0 & 0 & -N_in_x & N_in_y & 0 & N_in_y & N_in_x \end{pmatrix} l_b \tag{36}$$

For static analysis:

$$\tilde{\mathbf{K}}\mathbf{q} = \mathbf{F} \tag{37}$$

where $\mathbf{F}$ is the load vector defined as

$$\mathbf{F} = \int_\Omega \mathbf{p}\mathbf{N}d\Omega \tag{38}$$

For free vibration problems, we need to find $\omega \in \mathbf{R}^+$ such that

$$\left(\tilde{\mathbf{K}} - \omega^2\mathbf{M}\right)\mathbf{q} = 0 \tag{39}$$

where ω is the natural frequency and $\mathbf{M}$ is the global mass matrix given by

$$\mathbf{M} = \int_\Omega \mathbf{N}^T\mathbf{m}\mathbf{N}d\Omega \tag{40}$$

4. Numerical results

4.1. Static analysis

We consider a simply supported square laminated plate subjected to a sinusoidal load $P_z = q_0 \sin(\pi x/a)\sin(\pi y/b)$. The material properties of the plate are assumed $E_1 = 25E_2$; $G_{12} = G_{13} = 0.5E_2$; $G_{23} = 0.2E_2$; $v = 0.25$. The geometry data of problem are given as follows: the aspect ratio $a/b = 1$ and length-to-thickness ratios $a/h = 4, 10, 100$ for the sinusoidal load case. The non-dimensional displacements and stresses at the centroid of four layer $(0^\circ/90^\circ/90^\circ/0^\circ)$ square plate are defined as:

$$\bar{w} = \frac{100E_2h^3}{qa^4}w\left(\frac{a}{2},\frac{a}{2},0\right);\quad \bar{\sigma}_x = \frac{h^2}{qa^2}\sigma_1\left(\frac{a}{2},\frac{a}{2},\frac{h}{2}\right);\quad \bar{\sigma}_y = \frac{h^2}{qa^2}\sigma_2\left(\frac{a}{2},\frac{a}{2},\frac{h}{4}\right);$$
$$\bar{\sigma}_{xz} = \frac{h}{qa}\sigma_4\left(0,\frac{b}{2},0\right);\quad \bar{\sigma}_{yz} = \frac{h}{qa}\sigma_5\left(\frac{a}{2},0,0\right);\quad \bar{\sigma}_{xy} = \frac{h}{qa}\sigma_6\left(0,0,\frac{h}{2}\right);$$

Table 1. Non-dimensional displacement $\bar{w}$ and stresses $\bar{\sigma}$ of a supported simply $(0^\circ/90^\circ/90^\circ/0^\circ)$ square laminated plate under sinusoidal load

a/h	Methods	$\bar{w}$	$\bar{\sigma}_x$	$\bar{\sigma}_y$	$\bar{\sigma}_{xz}$	$\bar{\sigma}_{yz}$	$\bar{\sigma}_{xy}$
4	HSA4 [12]	1.9014	0.6973	0.6245	0.2112	0.2439	0.0456
	Reddy [8]	1.8937	0.6651	0.6322	0.2064	0.2389	0.0440
	NS-DSG3 [11]	1.9266	0.7076	0.6303	0.2084	0.2404	0.0475
	ES-DSG3 [10]	1.9046	0.7005	0.6236	0.2071	0.2387	0.0476
	Elasticity [9]	1.9540	0.7200	0.6660	0.2700	-	0.0467
	MISQ24-HSDT	1.9219	0.7019	0.6268	0.2126	0.2457	0.0458
10	HSA4 [12]	0.7190	0.5547	0.3872	0.2807	0.1580	0.0270
	Reddy [8]	0.7147	0.5456	0.3888	0.2640	0.1531	0.0268
	NS-DSG3 [11]	0.7246	0.5609	0.3909	0.2812	0.1566	0.0288
	ES-DSG3 [10]	0.7179	0.5554	0.3867	0.2793	0.1560	0.0288
	Elasticity [9]	0.7430	0.5590	0.4030	0.3010	-	0.0276
	MISQ24-HSDT	0.7264	0.5572	0.3889	0.2828	0.1592	0.0271
100	HSA4 [12]	0.4331	0.5333	0.2681	0.3114	0.1142	0.0211
	Reddy [8]	0.4343	0.5387	0.2708	0.2897	0.1117	0.0231
	NS-DSG3 [11]	0.4345	0.5384	0.2706	0.3183	0.1183	0.0211
	ES-DSG3 [10]	0.4310	0.5331	0.2680	0.3222	0.1365	0.0213
	Elasticity [9]	0.4347	0.5390	0.2710	0.3390	-	0.0214
	MISQ24-HSDT	0.4370	0.5352	0.2690	0.3138	0.1151	0.0212

The results of the present method are compared with several other methods such as finite element method (FEM) based on HSDT by Reddy [8], the elasticity solution 3D proposed by Pagano [9], the C^0-type higher order shear deformation theory by Loc et al. [10], finite element method based on HSDT and node-based smoothed discrete shear gap by Chien et al. [11], the a higher order shear deformation theory with assumed strains [12] as shown in Table 1. It is observed that the present results match very well with the exact solution [9]. The MISQ24-HSDT method gives the most accurate results for the all thin and thick plates. Figs. 3–6 plot the distribution of stresses through thickness plate with $a/h = 4$, 10 based on NS-DSG3 [11], ES-DSG3 [10], MISQ24-HSDT. It can be seen that the shear stresses vanish at boundary planes and distribute discontinuously through laminas.

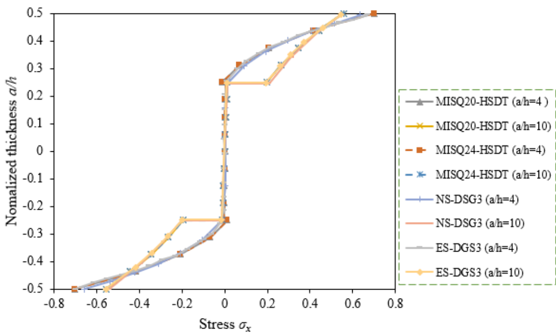

Figure 3. Distribution of stresses σ_x through thickness of plate under sinusoidally load with $a/h = 4, 10$ [10, 11]

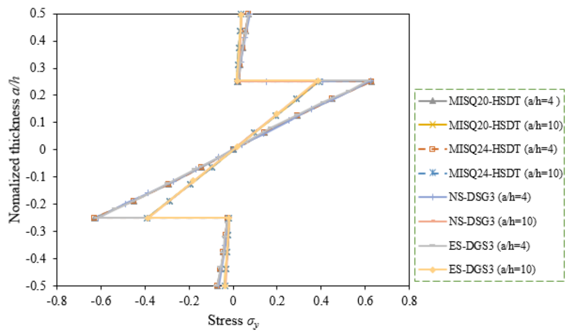

Figure 4. Distribution of stresses σ_y through thickness of plate under sinusoidally load with $a/h = 4, 10$ [10, 11]

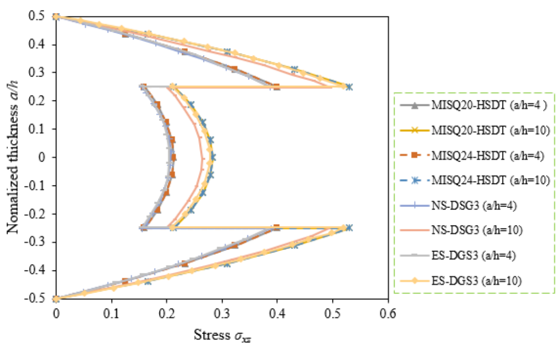

Figure 5. Distribution of shear stresses σ_{xz} through thickness of plate under sinusoidally load with $a/h = 4, 10$ [10, 11]

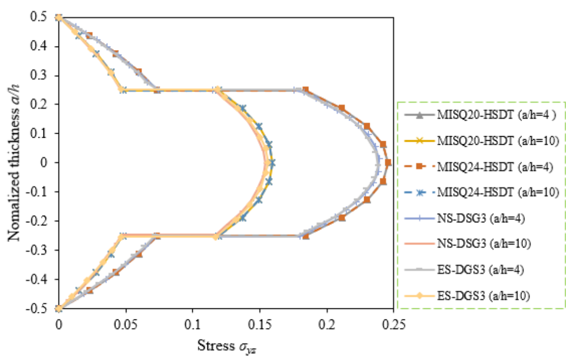

Figure 6. Distribution of shear stresses σ_{yz} through thickness of plate under sinusoidally load with $a/h = 4, 10$ [10, 11]

Next, we consider a simply supported square (0°/90°/0°) laminated plate subjecting to a sinusoidal load $P_z = q_0 \sin(\pi x/a) \sin(\pi y/b)$. The material properties of plate are assumed as $E_1 = 25E_2$; $G_{12} = G_{13} = 0.5E_2$; $G_{23} = 0.2E_2$; $\nu = 0.25$. The normalized displacement $\bar{w} = 100wEh^3/\left(qa^4\right)$, normal in-plane stresses $\bar{\sigma} = \sigma h^2/\left(qa^2\right)$ transverse shear stresses $\bar{\tau} = \tau h^2/(qa)$ are presented in Table 2. The study is made for the aspect ratio ($b/a = 3$) with various thickness ratio (a/h) such as 4, 10 and 100. In all the cases the analysis is done with three different types of mesh and the deflection and stress components obtained at the important locations are presented with the analytical solution of Reddy [8] in Table 2. The present results agree well with those of [8, 9, 13], especially for thick plates and compared with the solution finite element method based on HSDT by Reddy [8], the solution of 3D elasticity results [9], the solution of the MISQ24-HSDT is slightly nearer than those of Chakrabarti [13].

Table 2. Non-dimensional displacement $\bar{w}$ and stresses $\bar{\sigma}$ of a simply supported $(0°/90°/0°)$ square laminated plate under sinusoidal load $(b/a = 3)$

a/h	Methods	Mesh	$\bar{w}$	$\bar{\sigma}_x$	$\bar{\sigma}_y$	$\bar{\sigma}_{xz}$	$\bar{\sigma}_{yz}$	$\bar{\sigma}_{xy}$
4	Reddy [8]	16 × 16	2.6411	1.0356	0.1028	0.2724	0.0348	0.0263
	Pagano [9]		2.8200	1.1000	0.1190	0.3870	0.0334	0.0281
	Chakrabarti [13]		2.6437	1.0650	0.1209	0.2723	0.0320	0.0264
	MISQ24-HSDT		2.6785	1.0765	0.1168	0.2780	0.0324	0.0262
10	Reddy [8]	16 × 16	0.8622	0.6924	0.0398	0.2859	0.0170	0.0115
	Panago [9]		0.9190	0.7250	0.0435	0.4200	0.0152	0.0123
	Chakrabarti [13]		0.8649	0.7164	0.0383	0.2851	0.0106	0.0117
	MISQ24-HSDT		0.8770	0.7081	0.0450	0.3056	0.0158	0.0116
100	Reddy [8]	16 × 16	0.5070	0.6240	0.0253	0.2886	0.0129	0.0083
	Panago [9]		0.5080	0.6240	0.0253	0.4390	0.0108	0.0083
	Chakrabarti [13]		0.5097	0.6457	0.0253	0.2847	0.0129	0.0084
	MISQ24-HSDT		0.5104	0.6202	0.0283	0.3121	0.0120	0.0082

4.2. Free vibration analysis

a. Skew plate

In this example, we study the five-layer skew laminated $(45°/-45°/45°/-45°/45)$ square plates with simply supported and clamped condition boundary as shown in Fig. 7. In this problem, various skew angles are considered. The length-to-thickness ratio a/h is taken to be 10. The normalized frequencies are defined by $\bar{\omega} = \left(\omega b^2/\pi^2 h\right)(\rho/E_2)^{1/2}$ For comparison, the plate is modeled with 17 × 17 nodes. The normalized frequencies of the MISQ24-HSDT element with various skew angles from 0° to 60° are depicted in Table 3 corresponding with $(45°/-45°/45°/-45°/45)$ laminated skew plates, respectively. MLSDQ method by Liew et al. [14], radial basis approach reported by Ferreira et al. [15] and B-spline method by Wang [16]. It is again found that the obtained solutions are in good agreement with other existing ones for both cases of cross-ply laminates.

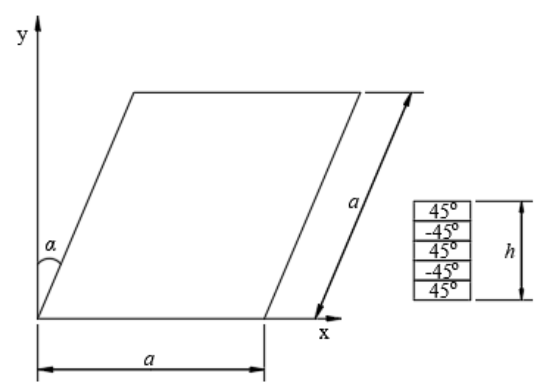

Figure 7. Geometry of skew laminated plate

Table 3. Non-dimensional fundamental frequencies $\bar{\omega} = \left(\omega b^2/\pi^2 h\right)(\rho/E_2)^{1/2}$ of simply supported and clamped cross-ply $(45°/-45°/45°/-45°/45)$ skew plate with various skew angles

Boundary	Methods	α				
		0	15	30	45	60
SSSS	MLSDQ [14]	1.8248	1.8838	2.0074	2.5028	4.0227
	RBF [15]	1.8357	1.8586	2.0382	2.4862	3.8619
	B-spline [16]	1.8792	-	2.0002	2.4788	-
	MISQ24-HSDT	1.8235	1.8550	2.0540	2.5590	3.9715
CCCC	MLSDQ [14]	2.2787	2.3504	2.6636	3.3594	4.8566
	RBF [15]	2.3324	2.3962	2.6981	3.3747	4.8548
	B-spline [16]	2.2857	-	2.6626	3.3523	-
	MISQ24-HSDT	2.2685	2.3052	2.5838	3.2349	4.6987

b. Triangular plate

In this example, we consider a clamped triangular plate. The following material properties are used in the analysis: $E_1/E_2 = 25; G_{12} = G_{13} = 0.5E_2; G_{23} = 0.5E_2; \nu_{12} = 0.25$ and $\rho = 1$. Table 4 shows a comparison of frequency parameter $\bar{\omega}$ using the present element with the solutions using LS12 higher-order element of Haldar and Sengupta [17], NS-DSG3 element [11] and Aα-DSG3 element [18] based on FSDT. The present results are compared well with those of other methods.

Table 4. Non-dimensional frequency parameter $\bar{\omega} = \left(\omega a^2/h\right)(\rho/E_2)^{1/2}$ of the (0°/90°/0°) triangle clamped laminated plate, $E_1/E_2 = 25$ and $a/h = 100$

Methods	Modes					
	1	2	3	4	5	6
Aα-DSG3 [18]	70.7200	109.7210	147.3460	161.2160	202.2890	221.8850
LS12 [17]	69.2520	106.7300	143.8800	155.0600	193.8400	210.1100
NS-DSG3 [11]	68.9609	107.1361	144.2034	157.7348	198.2622	217.4786
MISQ24-HSDT	69.5628	108.0224	146.0159	158.7462	200.0675	218.4925

5. Conclusions

In this paper, the MISQ24 element is further developed and successfully applied to static and free vibration analysis of composite plate structures in the framework of the C^0-HSDT model. The C^0-HSDT model provided more accurate solutions without shear correct factors. It is also noticed that the MISQ24 element associated with the C^0-HSDT only uses bilinear function approximations and does not require high computational cost as compared with other finite element models cited here. Numerical examples have been carried out and the present element is found to be free of shear locking and to yield satisfactory results in comparison with other published solutions in the literature.

References

[1] Clough, R. W., Tocher, J. L. (1964). Analysis of thin arch dams by the finite element method. In *Proc. Symp. Theory of Arch Darns, Southampton University*, 107–122.

[2] Zienkiewicz, O. C., Parekh, C. J., King, I. P. (1965). Arch dams analysed by a linear finite. In *Proc. Symp. Arch Dams, Pergamon Press, Oxford*.

[3] Providas, E., Kattis, M. A. (2000). An assessment of two fundamental flat triangular shell elements with drilling rotations. *Computers & Structures*, 77(2):129–139.

[4] Thanh, C. D., Con, H. T., Binh, L. P. (2019). Static analysis of Reissner-Mindlin plates using ES+ NS-MITC3 elements. *Journal of Science and Technology in Civil Engineering (STCE)-NUCE*, 13(3):45–57.

[5] Shankara, C. A., Iyengar, N. G. R. (1996). A C^0 element for the free vibration analysis of laminated composite plates. *Journal of Sound and Vibration*, 191(5):721–738.

[6] Nguyen-Van, H., Mai-Duy, N., Karunasena, W., Tran-Cong, T. (2011). Buckling and vibration analysis of laminated composite plate/shell structures via a smoothed quadrilateral flat shell element with in-plane rotations. *Computers & Structures*, 89(7-8):612–625.

[7] Ibrahimbegovic, A., Taylor, R. L., Wilson, E. L. (1990). A robust quadrilateral membrane finite element with drilling degrees of freedom. *International Journal for Numerical Methods in Engineering*, 30(3): 445–457.

[8] Reddy, J. N. (1984). A simple higher-order theory for laminated composite plates. *Journal of Applied Mechanics*, 51(4):745–752.

[9] Pagano, N. J. (1994). Exact solutions for rectangular bidirectional composites and sandwich plates. *Mechanics of Composite Materials*, 86–101.

[10] Loc, T. V., Chien, T. H., Dung, T. T., Hung, N. X. (2012). Static and dynamic analysis of composite plate using the C^0-type higher-order shear deformation theory. *Journal of Science HCMC Open University*.

[11] Thai, C. H., Tran, L. V., Tran, D. T., Nguyen-Thoi, T., Nguyen-Xuan, H. (2012). Analysis of laminated composite plates using higher-order shear deformation plate theory and node-based smoothed discrete shear gap method. *Applied Mathematical Modelling*, 36(11):5657–5677.

[12] Lee, S. J., Kim, H. R. (2013). FE analysis of laminated composite plates using a higher order shear deformation theory with assumed strains. *Latin American Journal of Solids and Structures*, 10(3):523–547.

[13] Sheikh, A. H., Chakrabarti, A. (2003). A new plate bending element based on higher-order shear deformation theory for the analysis of composite plates. *Finite Elements in Analysis and Design*, 39(9): 883–903.

[14] Liew, K. M., Huang, Y. Q., Reddy, J. N. (2003). Vibration analysis of symmetrically laminated plates based on FSDT using the moving least squares differential quadrature method. *Computer Methods in Applied Mechanics and Engineering*, 192(19):2203–2222.

[15] Ferreira, A. J. M., Roque, C. M. C., Jorge, R. M. N. (2005). Free vibration analysis of symmetric laminated composite plates by FSDT and radial basis functions. *Computer Methods in Applied Mechanics and Engineering*, 194(39-41):4265–4278.

[16] Wang, S. (1997). Free vibration analysis of skew fibre-reinforced composite laminates based on first-order shear deformation plate theory. *Computers & Structures*, 63(3):525–538.

[17] Haldar, S., Sengupta, D., Sheikh, A. H. (2003). Free vibration analysis of composite right angle triangular plate using a shear flexible element. *Journal of Reinforced Plastics and Composites*, 22(3):229–255.

[18] Thai-Hoang, C., Nguyen-Thanh, N., Nguyen-Xuan, H., Rabczuk, T. (2011). An alternative alpha finite element method with discrete shear gap technique for analysis of laminated composite plates. *Applied Mathematics and Computation*, 217(17):7324–7348.